

Development of a HBV tripler for 0.6 THz

Johanna Liljedahl*, Tomas Bryllert, Josip Vukusic and Jan Stake

Dept. of Microtechnology and Nanoscience, Chalmers University of Technology, Göteborg, Sweden

*Contact: johanna.liljedahl@chalmers.se, phone +46(0)31 772 18 75

Abstract—We report on the progress of the design of a HBV frequency tripler for 0.6 THz. The diode is based on the InGaAs/InAlAs/AlAs on InP material system, and the diode material and geometry has been optimised with regards to conversion efficiency. In designing the diode, it was found that self heating is the major limiting factor due to the poor thermal conductivity of InGaAs. The resulting HBV is a two-mesa diode from a three-barrier material, with a mesa area of $6 \times 3 \mu\text{m}^2$, and is estimated to have a 6-7% conversion efficiency and 100 - 150 K self heating at an input power of 30 mW.

I. INTRODUCTION

The trend in recent space observing projects is to cover frequencies in the terahertz (THz) gap. In many observing applications the high spectral resolution from heterodyne receivers is desired. However, when going from millimetre to sub-millimetre wavelengths there is a lack of fundamental LO sources above 200 GHz. Therefore the most commonly used and efficient solution for LO signal sources is frequency up-conversion through multiplication by non-linear semiconductor devices [1].

Today most frequency multiplier circuits are realized using Schottky diodes. Due to their high performance, balanced Schottky doublers have become standard as multiplier sources, and planar Schottky diode multipliers for the THz frequency range have been demonstrated [2].

An alternative to the Schottky diode is the Heterostructure Barrier Varactor (HBV). Ever since the invention in 1989, the HBV diode has been promising for frequency multiplication to THz frequencies [3]. Today HBV diodes are used as high power multipliers for frequencies up to and above 200 GHz [4].

The HBV consists of a wide bandgap semiconductor barrier spaced between two narrow bandgap, equally doped, semiconductor modulation layers. The C-V curve is symmetric, while the I-V curve is anti-symmetric, and these properties cause the HBV to only generate odd harmonics. Thereby, when used as a frequency tripler, there is only need for circuit matching at the in and output frequencies, and no idler matching is needed. In addition, there is no need for DC-biasing, which together with the matching requirements enables a simple and compact circuit design, making it ideal for space applications.

Another advantage is that the sandwich structure of the HBV allows stacking of several diodes for better power handling capability, and at the same time diode miniaturisation is prevented [5]. Nevertheless, the highest output frequency published for HBV diode based multipliers is 450 GHz [6]. Our aim is to push this limit further into the sub-mm region.

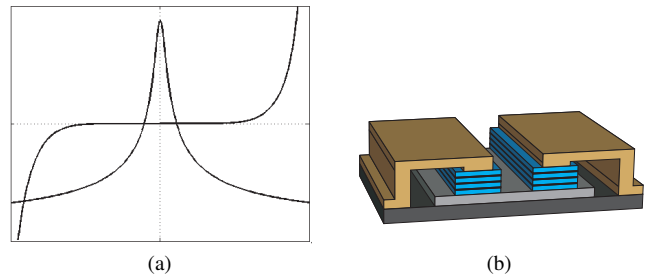


Fig. 1. (a) C-V and I-V curve for a HBV diode. C-V is symmetric while I-V is antisymmetric. (b) Model of a two-mesa HBV diode with a total of six barriers, and gold air bridges. (The model is not according to scale)

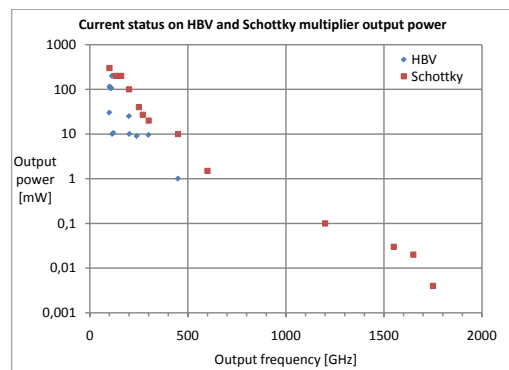


Fig. 2. Current status on output power for single diode HBV frequency multipliers and Schottky diode frequency multiplier chains [7][8][9][5].

We present the current status on the development of an HBV tripler for an output frequency of 600-700 GHz. The designed HBV is based on the InGaAs/InAlAs/AlAs epitaxially grown on InP material system. The doping and layer structure impact on the conversion efficiency has been evaluated, and consideration of the effects of self heating has been crucial when choosing an appropriate diode design. The HBV diode is implemented in a MMIC circuit containing matching and filtering elements.

II. 0.6 THz HBV TRIPLER DEVELOPMENT

In developing a 600 GHz frequency tripler there are several constraints to consider. At this high input frequency, 200-220 GHz, the available power is estimated to be less than 40 mW, which together with impedance boundaries limits the size and geometry of the diode. The high frequency makes it unsuitable for the otherwise commonly used flip chip soldering, hence the HBV frequency tripler is implemented using a monolithic

approach which offers high repeatability.

For the circuit design we decided to use conventional technology, with the advantage of having good heat sinking properties and already established designs to fall back on. The tripler will consist of a waveguide block, with waveguide in and outputs, and the matching circuit and HBV on a microstrip MMIC in a waveguide channel, coupled into the waveguides by probes.

We have limited ourselves to the use of the InGaAs/InAlAs/AlAs epitaxially grown on an InP substrate material system. The advantages of this material are the high mobility of InGaAs and the height of the energy bandgap barrier.

An effort to analytically optimise the material structure with regards to the conversion efficiency for an input frequency of 200 GHz has been made. This optimised material, material A was then compared to an already grown material, material B, to evaluate the necessity of growing a new material. The existing Material B has been verified in I-V and C-V measurements.

In comparing the two materials the effects of self heating were taken into account through FEM heat transfer modelling combined with harmonic balance simulations in ADS. In these simulations the diode geometry was investigated as well.

Finally the optimum embedding impedances for the HBV diode tripler configuration has been determined to maximise the conversion efficiency. For these simulations a 3-D model of the diodes including air bridges have been modelled in Ansoft HFSS for S-parameter extraction, combined with harmonic balance simulations in ADS.

III. MATERIAL VERIFICATION

The material in Table I, earlier introduced as Material B, has been verified in I-V and C-V measurements, see figure 3. For these measurements single mesa test diodes were fabricated with different areas and measured in a probe station with an I-V and a LCR meter. The maximum capacitance of the HBV material was measured to be $C_{max} = 0.9 \text{ fF}/\mu\text{m}^2$, and the breakdown voltage $V_{br} = \pm 19 \text{ V}$ (for 3 barriers). From the C-V measurements the doping concentration was extracted, $N_d = 1.4 \cdot 10^{17} \text{ cm}^{-3}$, which is slightly higher than the specification. The extracted value for the doping was then used when evaluating the material in harmonic balance simulations, described below.

IV. DIODE OPTIMISATION

The HBV tripler will be pumped with at a frequency of 200-220 GHz, and at this frequency the expected available input power is about 20-40 mW. Thus the diode is optimised for an input power of 30 mW. Diode parameters such as the epi-layer structure, size and geometry have been examined in order to ensure large conversion efficiency. Furthermore, the advantage of growing a new frequency optimised material, versus using a material that has already been fabricated, but is optimised for a lower frequency range, has been evaluated.

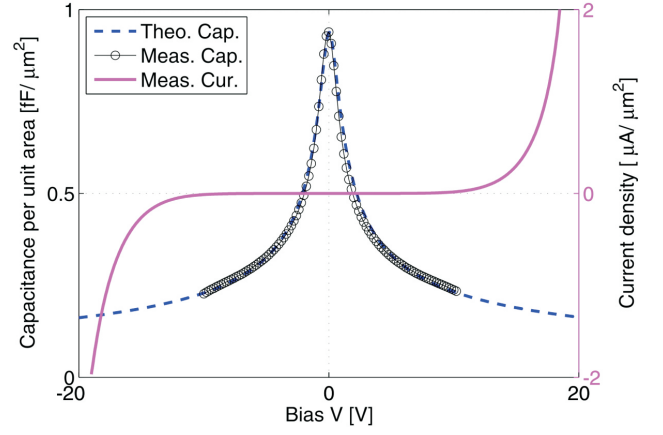


Fig. 3. I-V and C-V measurement result plus the theoretical C-V curve using the extracted doping.

A. Epi-layers

1) *Barrier*: The barrier material in the epi-layer design consists of a 3 nm thin layer of AlAs in the middle of two layers of 50 nm $\text{In}_{0.52}\text{Al}_{0.48}\text{As}$. The AlAs prevents leakage current by increasing the energy bandgap, but this barrier layer is lattice mismatched to InAlAs, so in order to keep it strained the thickness is limited. This optimum barrier design for the InGaAs/InAlAs/AlAs HBV material system is further described in [10] and [11], and has not been treated within this work.

2) *Modulation layers*: A figure of merit for a varactor diode design is the dynamic cut-off frequency [12]

$$f_c = \frac{S_{max} - S_{min}}{2\pi R_S} \quad (1)$$

It is derived from the equivalent circuit of a varactor with a variable reactance, $C(v) = \frac{1}{S(v)}$, connected in series with a resistance, R_S .

The cutoff frequency dependence of the conversion efficiency can be estimated by

$$\eta \approx \frac{100}{1 + \alpha \left(\frac{f_p}{f_c}\right)^\beta} \% \quad (2)$$

where f_p is the pumping frequency, f_c the cutoff frequency, $\alpha = 200$ and $\beta = 1.5$ [13]. So in order to achieve a high efficiency, the cutoff frequency should be maximised, which is done by maximising the difference in elastance and minimising the series resistance.

The series resistance consists of several resistance elements

$$R_S = R_{active} + R_{spread,buffer} + R_{contact} \quad (3)$$

where the resistance in the epi-layers is

$$R_{active} = \sum_n \frac{l_n}{\mu_n N_n q A} \quad (4)$$

n is the layer number, l_n the layer thickness, μ_n the layer mobility, N_n the layer doping and A the mesa area. The

spreading resistance between two mesas or mesa and contact for a single mesa diode is

$$R_{spread,buffer} = \frac{l_{buffer}}{\mu_{buffer} N_{buffer} q A_{buffer}} \quad (5)$$

and the ohmic contact resistance is

$$R_{contact} = N_m \frac{r_c}{A} \quad (6)$$

where N_m is the number of mesas and $r_c = 100 \Omega\text{-}\mu\text{m}^2$. The mobility is doping dependent and estimated according to [14].

The minimum elastance is determined by the Debye length, L_D ,

$$S_{min} = \frac{N}{A} \left(\frac{b}{\varepsilon_b} + \frac{2s}{\varepsilon_d} + \frac{2L_D}{\varepsilon_d} \right) \quad (7)$$

while the maximum elastance is determined by the maximum depletion width, w_{max} , [13]

$$S_{max} = \frac{N}{A} \left(\frac{b}{\varepsilon_b} + \frac{2s}{\varepsilon_d} + \frac{w_{max}}{\varepsilon_d} \right). \quad (8)$$

N is the number of barriers, A the diode area, b and s the barrier and spacer thickness respectively, and ε the dielectric constants for the different materials. The maximum depletion width is limited by impact ionization, which is doping dependent, and by the current saturation which can be approximated to be constant with regards to the doping level for a constant pumping frequency [13]. This means that for doping levels above a certain value the cutoff frequency is impact ionization limited and below that frequency it is limited by the current saturation. These two criteria can be combined to estimate the optimum doping level for a high cutoff frequency, see figure 4.

This model indicates that the difference in modulation layer thickness has little impact on the conversion efficiency compared to for example the number of barriers, i.e. HBV diodes stacked in series. In order to minimise the series resistance, an optimised modulation layer thickness has the same value as the maximum depletion width, and the cut-off frequency decreases for thicker layers. While the cut-off frequency increases with the number of barriers. However, as the number of barriers increase, so does the input power necessary to drive the HBV. Therefore we chose to compare conversion efficiency for HBV diodes with different geometries, made of a two-barrier material with a modulation layer thickness of 190 nm and doping of $1.4 \cdot 10^{17} \text{ cm}^{-3}$, i.e. Material A, and the three-barrier material we already have, Material B (see Table I).

B. Device geometry

In deciding the geometry of the HBV diode taking the effects of self heating into account is crucial due to the poor thermal conductivity of InGaAs. Using heat transfer FEM simulations combined with ADS harmonic balance simulations the heating in the diode active region and the conversion efficiency has been estimated, and an appropriate geometry found.

TABLE I
HBV ACTIVE LAYER MATERIAL SPECIFICATION, MATERIAL B

Layer	Material	Thickness [Å]	Doping [cm^{-3}]	Comment
1	In _{0.53} Ga _{0.47} As	2,500	10^{17}	Modulation
2	In _{0.53} Ga _{0.47} As	50	Undoped	Spacer
3	In _{0.52} Al _{0.48} As	50	Undoped	Barrier
4	AlAs	30	Undoped	Barrier
5	In _{0.52} Al _{0.48} As	50	Undoped	Barrier
6	In _{0.53} Ga _{0.47} As	50	Undoped	Spacer
7-18	... 2 × Layers 1 - 6 ...			
19	In _{0.53} Ga _{0.47} As	2,500	10^{17}	Modulation

1) *Self heating*: In the FEM heat transfer model the power distributed as a volume power source, assuming all input power is converted to heat, see Figure 5. The resulting temperature is then used to calculate the thermal resistance, R_T of the diode, and the thermal resistance is then put in to ADS harmonic balance simulations where self heating is implemented using Chalmers HBV electro-thermal model to calculate the rise in temperature under RF pumping [15]. In the heat transfer simulations the temperature dependent thermal conductivity is used for InGaAs, InP and gold.

$$\begin{aligned} \kappa_{InGaAs} &= 4.7 \cdot \left(\frac{T_0}{T} \right)^{1.375} \\ \kappa_{InP} &= 68 \cdot \left(\frac{T_0}{T} \right)^{1.48} \\ \kappa_{Au} &= 0.0586(282 - T) + 317 \end{aligned}$$

2) *Harmonic balance*: The electrical properties of the HBV are modeled in ADS with the quasi-empirical Chalmers HBV model [16]

$$V(Q) = N \left\{ \frac{bQ}{\varepsilon_b A} + 2 \frac{sQ}{\varepsilon_d A} + \text{Sign}(Q) \cdot \left(\frac{Q^2}{2qN_d \varepsilon_d A^2} + \frac{4k_B T}{q} \left(1 - \exp \left[-\frac{|Q|}{2L_D A q N_d} \right] \right) \right) \right\} \quad (9)$$

These simulations also provides a value for the optimum embedding impedances for a maximised conversion efficiency.

Different geometries have been evaluated for a fixed input power of 40 mW and pump frequency $f_p = 200 \text{ GHz}$. We have examined one and two-mesa HBV diodes, with different mesa areas, of Material A and B, to determine which geometry will give the highest conversion efficiency without exceeding the maximum temperature increase allowed, 130 – 150 K. For each geometry the efficiency improves when the area decreases, see Figure 6. However only the geometry and areas where the temperature limit has not been reached are interesting, consequently the one-mesa geometry could be ruled out immediately since the area required results in a very low conversion efficiency of the HBV diode.

The best conversion efficiency geometry was chosen, a two-mesa HBV with a mesa area of $6 \times 3 \mu\text{m}^2$, where the larger dimension sets the width of the air bridges. As can be seen in figure 6, the difference in efficiency is not very large, why we choose to use the epi-material we already have, Material B, rather than fabricate a new material.

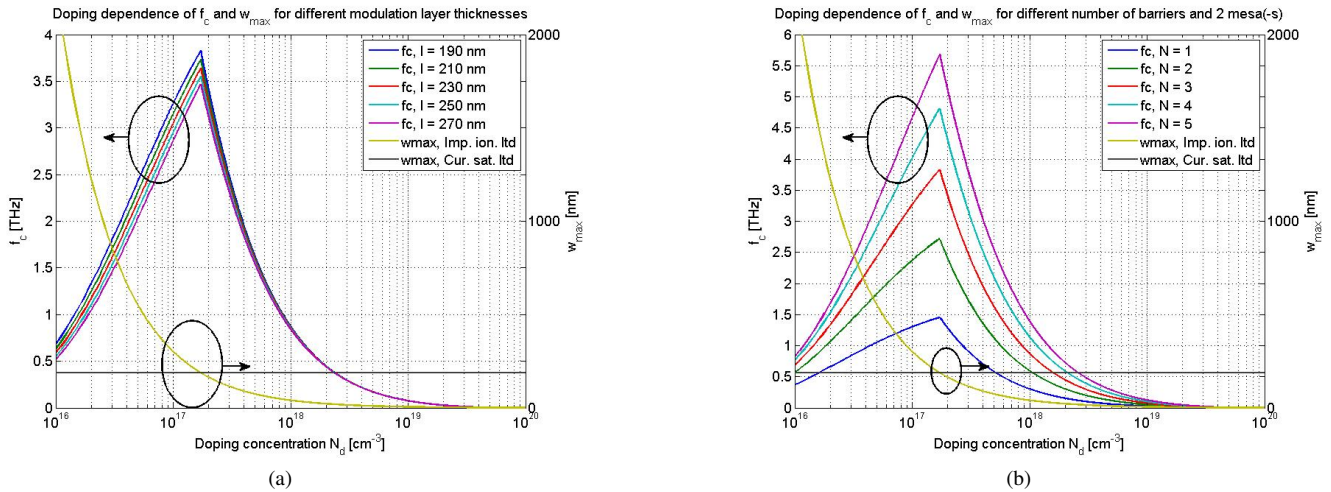


Fig. 4. Cutoff frequency and maximum depletion layer width dependence on modulation layer doping level. To the left of the intersection the cutoff frequency is current saturation limited, and to the right the cutoff frequency is impact ionization limited. $f_p = 200$ GHz, $A = 18 \mu m^2$. (a) Cutoff frequency for different thickness of the modulation layers. $N = 3$, $N_m = 2$. (b) Cutoff frequency for different number of barriers per mesa. $l = 190$ nm, $N_m = 2$.

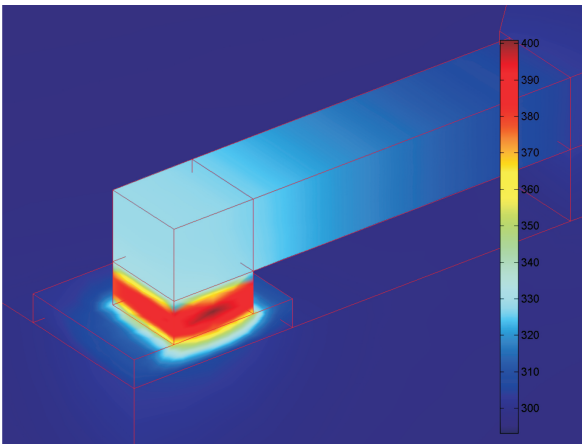


Fig. 5. Heat transfer FEM simulation of a two-mesa HBV diode. Clearly shows how the heat is concentrated in the active layers of the HBV. The image shows quarter of a diode, due to symmetry.

V. CIRCUIT

While HBV diodes for lower frequencies often are separately flip chip soldered to a circuit of another material, e.g. quartz, integration of the HBV diode on a MMIC is preferable for THz frequencies. As the frequency gets higher soldering uncertainty and losses are eliminated. This means that we are limited to a InP substrate which has a large dielectric constant, so in order to reach reasonable line widths and impedances, and to avoid waveguide modes in the substrate, the substrate needs to be thin.

We will design a classic waveguide-to-microstrip-to-waveguide circuit, with all matching elements fabricated on the microstrip MMIC. The waveguide dimensions are WR-4 at the input and WR-1.5 at the output. The channel width and height is $160 \mu m$. The design is similar to the design in [17].

A. Substrate

The most common way to thin down a substrate is either mechanically, through lapping of the back of the substrate, or through membrane technology where the back side of the substrate is etched away until a stop layer is reached deciding the substrate thickness. As InP is a brittle material there is some concern when thinning it down too thin. And as for membrane technology there are also some issues regarding the background doping of the epitaxially grown InP layer. We do not have access to Fe-doped InP epi-material, which means the membrane will be lossy.

We have decided to move forward with a $20 \mu m$ thick substrate, which we can lap down mechanically with good precision. Propagation constant simulations in Ansoft HFSS show that $20 \mu m$ is small enough to avoid waveguide modes in the substrate for strip widths smaller than about $40 \mu m$ in a waveguide $160 \mu m$ wide, but still large enough to have a reasonable tolerance.

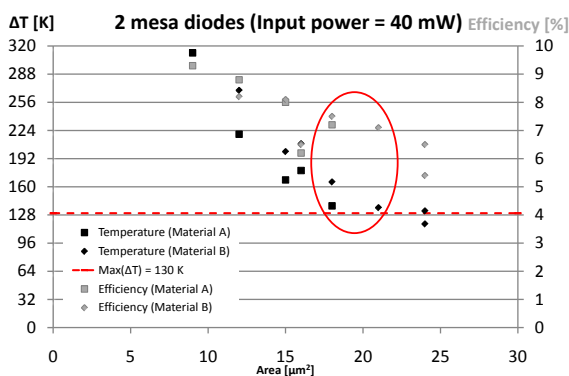


Fig. 6. Efficiency and temperature comparison of two-mesa diodes with different mesa areas and two different materials: A two-barrier material optimised for an input frequency of 200 GHz, and the 3-barrier material described in Table I. It shows that the area needs to be at least $18 \mu m^2$ to not overheat, and that the 3-barrier material we already have can be used.

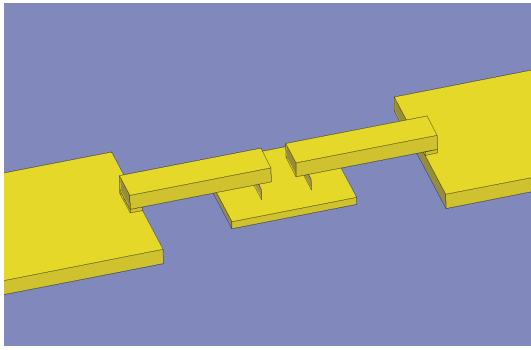


Fig. 7. HBV diode HFSS model with airbridges for deembedding optimum impedances.

B. Diode embedding impedance

The optimum HBV diode embedding impedance has been estimated in order to achieve maximum conversion efficiency at an input power of 30 mW in order to keep good efficiency over the whole 20–40 mW region. The input and output matching impedance for the fundamental tone at 200 GHz and third harmonic has been calculated in S-parameter simulations in Ansoft HFSS combined with harmonic balance simulations in ADS of the chosen geometry, a two-mesa diode of the three-barrier material (Material B). The air bridges are included in the S-parameter simulation, see Figure 7, in order to have them included in future matching circuit simulations. The HBV diode mesas are replaced with lumped ports in this simulation, and the HBV model in (9) is used in ADS. The length of the air bridges is $12 \mu\text{m}$, the width is $4 \mu\text{m}$, the mesa area is $6 \times 3 \mu\text{m}^2$, the distance between the mesas is $3 \mu\text{m}$, pump frequency $f_p = 200 \text{ GHz}$ and the input power is 30 mW. The thermal resistance put in to the device is a "worst case" thermal resistance calculated from an input power of 40 mW on the same diode area, $R_T = 4474 \text{ K/W}$.

The resulting optimum impedances at the fundamental and third harmonic, for an input frequency of 200 GHz is displayed in Figure 8. The conversion efficiency at these impedances is $\eta > 6\%$ and the self heating in the HBV diode is $100 < \Delta T < 150 \text{ K}$.

VI. CONCLUSION

A HBV frequency tripler with an output frequency of 0.6 THz is currently under development. Investigations of material and diode layout show that self heating is a major limiting factor for reaching high conversion efficiency and power levels at higher frequencies. The 3-barrier epi-material developed for operation at lower frequencies can be used for the HBV and provide a theoretical conversion efficiency of 6-7% for a 2-mesa HBV diode. At an expected input power of 30 mW this will result in a output power of about 1 mW.

The circuit developed for the tripler is a waveguide-to-microstrip MMIC-to-waveguide circuit. The matching circuitry on the MMIC is under development and when that is done the HBV tripler will be fabricated at MC2, Chalmers.

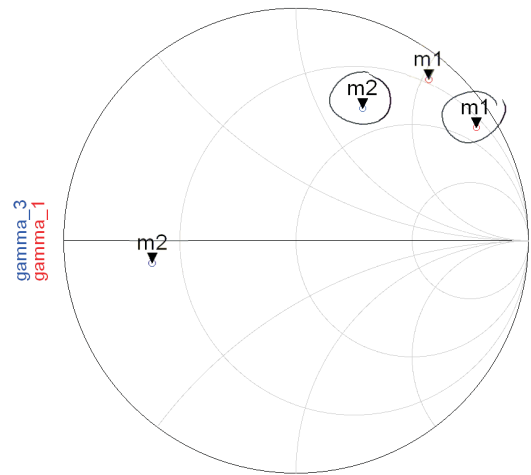


Fig. 8. HBV optimum embedding impedances for maximised efficiency at 30 mW input power and $f_p = 200 \text{ GHz}$. $m1$ marks the input matching impedance for fundamental tone, and $m2$ the output impedance at the third harmonic including and excluding (circled) air bridges.

ACKNOWLEDGMENT

The authors would like to thank the Swedish Research Council (VR) and MSB "ISSI" for funding this research.

REFERENCES

- [1] P. H. Siegel, "THz Technology: An Overview," *International Journal of High Speed Electronics and Systems*, vol. 13, no. 2, pp. 351–394, 2003.
- [2] A. Maestrini, J. Ward, J. Gill, H. Javadi, E. Schlecht, C. Tripon-Canseliet, G. Chattopadhyay, and I. Mehdi, "A 540-640-ghz high-efficiency four-anode frequency tripler," *Microwave Theory and Techniques, IEEE Transactions on*, vol. 53, no. 9, pp. 2835 – 2843, sept. 2005.
- [3] E. Kollberg and A. Rydberg, "Quantum-Barrier-Varactor Diodes for High-Efficiency Millimetre-Wave Multipliers," *Electronic Letters*, vol. 25, no. 25, pp. 1696–1698, 1989.
- [4] J. Stake, T. Bryllert, A. i. Olsen, and J. Vukusic, "Heterostructure barrier varactor quintuplers for terahertz applications," *Proceedings of the 3rd European Microwave Integrated Circuits Conference*, pp. 206 – 209, oct. 2008.
- [5] J. Vukusic, T. Bryllert, T. A. Emadi, M. Sadeghi, and J. Stake, "A 0.2-W heterostructure barrier varactor frequency tripler at 113 GHz," *IEEE ELECTRON DEVICE LETTERS*, vol. 28, no. 5, pp. 340–342, MAY 2007.
- [6] M. Saglam, B. Schumann, V. Mullerwiebus, A. Megej, U. Auer, M. Rodriguez-Girones, R. Judaschke, E. Tegude, and H. Hartnagel, "450 ghz millimetre-wave signal from frequency tripler with heterostructure barrier varactors on gold substrate," *Electronics Letters*, vol. 38, no. 13, pp. 657 –658, Jun 2002.
- [7] J. S. Ward, G. Chattopadhyay, J. Gill, H. Javadi, C. Lee, R. Lin, A. Maestrini, F. Maiwald, I. Mehdi, E. Schlecht, and P. Siegel, "Tunable broadband frequency-multiplied terahertz sources," *Infrared, Millimeter and Terahertz Waves, 2008. IRMMW-THz 2008. 33rd International Conference on*, pp. 1 – 3, sept. 2008.
- [8] J. Stake, T. A. Emadi, and J. Vukusic, "Terahertz generation by multiplication," in *Terahertz Frequency Detection and Identification of Materials and Objects*, R. E. Miles, X.-C. Zhang, H. Eisele, and A. Krotkus, Eds. Dordrecht, The Netherlands: Springer Netherlands, 2007, pp. 17–30.
- [9] V. D. Inc., "Multipliers," available: <http://www.virginiadiodes.com/>, Date: April 13 2010.
- [10] Y. Fu, J. Stake, L. Dillner, M. Willander, and E. L. Kollberg, "Al-GaAs/GaAs and InAlAs/InGaAs heterostructure barrier varactors," *Journal of Applied Physics*, vol. 82, no. 11, pp. 5568–5572, Dec 1997.
- [11] T. A. Emadi, T. Bryllert, M. Sadeghi, J. Vukusic, and J. Stake, "Optimum barrier thickness study for the InGaAs/InAlAs/AlAs heterostructure barrier varactor diodes," *Applied Physics Letters*, vol. 90, no. 1, Jan 2007.
- [12] P. J. Penfield and R. P. Rafuse, *Varactor Applications*. The M.I.T. Press.

- [13] J. Stake, S. H. Jones, L. Dillner, S. Hollung, and E. L. Kollberg, "Heterostructure-Barrier-Varactor Design," *IEEE Transactions on Microwave Theory and Techniques*, vol. 48, no. 4, pp. 677–682, Apr 2000.
- [14] M. Sotoodeh, A. Khalid, and A. Rezazadeh, "Empirical low-field mobility model for III-V compounds applicable in device simulation codes," *JOURNAL OF APPLIED PHYSICS*, vol. 87, no. 6, pp. 2890–2900, MAR 15 2000.
- [15] M. Ingvarson, J. Vukusic, A. Olsen, T. Emadi, and J. Stake, "An electro-thermal HBV model," in *2005 IEEE MTT-S INTERNATIONAL MICROWAVE SYMPOSIUM, VOLS 1-4*, 2005, pp. 1151–1153.
- [16] L. Dillner, J. Stake, and E. Kollberg, "Modeling of the heterostructure barrier varactor diode," 1997, presented at the Int. Semiconductor Device Res. Symp., Charlottesville, VA.
- [17] J. Vukusic, A. Ø. Olsen, T. Bryllert, and J. Stake, "High power w-band monolithically integrated tripler," *International Conference on Infrared, Millimeter, and Terahertz Waves IRMMW 2009 Proceedings*, 2009.